The Effect of Mobile Polymers on the Normal and Shear Forces between Polymer Brushes

Erika Eiser*,† and Jacob Klein*,‡

Van t'Hoff Institute for Molecular Sciences, University of Amsterdam, Nieuwe Achtergracht 166, 1018WV Amsterdam, The Netherlands, Physical & Theoretical Chemistry Laboratory, South Parks Road, Oxford OX1 3QZ, United Kingdom, and Weizmann Institute of Science, Rehovot 76100, Israel

Received May 2, 2007; Revised Manuscript Received August 17, 2007

ABSTRACT: We used the surface force balance technique to investigate the influence of free polymer chains on the equilibrium and dynamic properties of dense polymer brushes, focusing on their extension and swelling under oscillatory shear flow. In particular, we extend earlier results on shear of brushes (*Nature* **1991**, *352*, 413) both to additional molecular weights of the brush and especially, for the first time, to the effect of the added free polymer. We present experimental studies on how the equilibrium properties of these polymer brushes are influenced by the presence of free, chemically identical polymer chains well above the overlap concentration, $c \approx 40-50\ c^*$. We observe a strong influence of the free chains on the behavior of the brushes when high shear rates are applied, even when the brushes are well away from contact, indicating a clear coupling between the brush and the free polymer. The onset of shear-induced swelling in our experiments correlates reasonably well with the relaxation properties of the outer regions of the brushes.

1. Introduction

Polymer brushes have long been recognized as efficient modifiers of both equilibrium and dynamic properties of surfaces, and extensive experimental[1−6] and theoretical[7,8] studies on end-grafted polymers in good solvent conditions have led to a reasonably good understanding of their properties. Experiments to measure friction between brush-covered surfaces revealed that surfaces protected by polymer brushes resulted in very efficient wet lubrication at moderate shear rates and loads.[9,10] In a different type of shear study, Klein et al.[3] showed that when two mica surfaces densely covered with polystyrene brushes immersed in toluene (a good solvent) were sheared above a critical shear rate, $\dot{\gamma}$, shear-induced swelling of the brush occurred. This was subsequently investigated widely. Several theoretical studies[11−13,41] and a Brownian dynamics study by Doyle et al.[15] on steady and oscillatory shear support the existence of shear-induced brush swelling. However, neutron reflectivity measurements[16,17] and other theoretical[14] and simulation studies[18−23] on steady shear past a single brush layer in good solvent do not show such swelling. The picture emerging from these studies is that polymer brushes in good solvent conditions appear to respond to high shear rates with stretching and tilt of the polymers, but under steady-state shear (as opposed to oscillatory shear), the net brush thickness may not increase.

Here we report how swollen polymer brushes behave in the presence of free chains chemically identical to the brush. We study both the static brush height and how it changes at large shear rates. Little is known about the effect of free nonadsorbing polymer on the configuration of the polymer brush and its lubrication properties.[24−26] Wetting experiments by Yerushalmi-Rozen and Klein[27] show that polymer brushes in combination with long free chains can stabilize thin liquid films that otherwise rupture and finally completely dewet a solid surface. This suggests that the free polymer is coupled to the brush creating a network that promotes the stability of the film.[28] To gain more insight into this coupling mechanism, we measured the normal and shear forces between two brush-covered surfaces as a function of their separation. We compare the results with those obtained when free polymer is present. Using a special design of the surface force balance, SFB, allowed us also to investigate the shear behavior of brushes at very high shear velocities, where we observe brush swelling, in agreement with earlier work.[3] This may also have an interesting application as pressure-sensitive microvalves, as suggested by Sevick and Williams.[29] In general, normal force and shear studies are of importance for the understanding of polymeric lubricants and the rheological behavior of stabilized dispersions and multiphase polymeric systems.

In the following section, we first present the new SFB design first used by us in an earlier study[30,31] and discuss its particular features. In Section 3, we present our experimental results: for clarity, we separate the normal force measurements from the data obtained for the coupling between shear and normal forces. Finally, a discussion of the results will follow, with particular emphasis on trying to understand the results in terms of molecular models, and on attempting to reconcile the neutron-reflectometry studies[16,17] on brushes in monotonic shear with the present results.

2. Experimental Section

Materials. The brushes were composed of linear polystyrene with one zwitterionic end group, $-X$, $-(CH_2)_3N^+(CH_2)_3-(CH_2)_3-SO_3^-$ (kindly provided by L.J. Fetters; see Taunton et al.[32]). We refer to these end-functionalized chains as PS−X(M_w), where M_w specifies the weight-average molecular weight, given together with other molecular characteristics in Table 1. For the free polymer, we used unfunctionalized linear polystyrene, PS, purchased from Polymer Laboratories (U.K.) (Table 1). In all experiments, spectroscopic grade toluene, purchased from Sigma, was used as received. Toluene is a good solvent for PS.

Experimental Method. In Figure 1, we illustrate the surface force balance we used. Similar to the SFB described earlier,[3,33] we

* Corresponding authors. E-mail: eiser@science.uva.nl (E.E.); jacob.klein@weizmann.ac.il (J.K.).
† Van t'Hoff Institute for Molecular Sciences, University of Amsterdam.
‡ Physical & Theoretical Chemistry Laboratory, South Parks Road, Oxford OX1 3QZ, United Kingdom, and Weizmann Institute of Science, Rehovot 76100, Israel.

10.1021/ma071000n CCC: $37.00
Published on Web 10/18/2007

Table 1

sample	M_w,[a] g/mol	R_F,[b] Å	$2L_0$,[c] Å	c^*,[d] mg/mL	ξ_0,[e] Å
PS−X (26K)	26 000	122	430 ± 50	5.67	47
PS−X (140K)	140 000	323	1400 ± 100	2.93	85
PS−X (370K)	370 000	575	2450 ± 100	1.39	143
PS (1.46 M)	1 460 000	1292		0.268	

[a] The polydispersity M_w/M_n is 1.04 for the PS and 1.03 for the PS−X samples. [b] Unperturbed Flory end-to-end distance in good solvent conditions: $R_F = 0.32\ M_w^{0.585}$. [c] $2L_0$: Mean surface separation at the onset of detected repulsion (equilibrium thickness of the brush). [d] Overlap concentration calculated from the relation $c^* = (M_w/R_F^3)/((4/3)\pi N_A)$,where N_A is Avogadro's number. [e] The blob size ξ_0 is here assumed to be equal to the mean interanchor spacing s between PS−X chains grafted to mica (taken from Taunton et al.[32]).

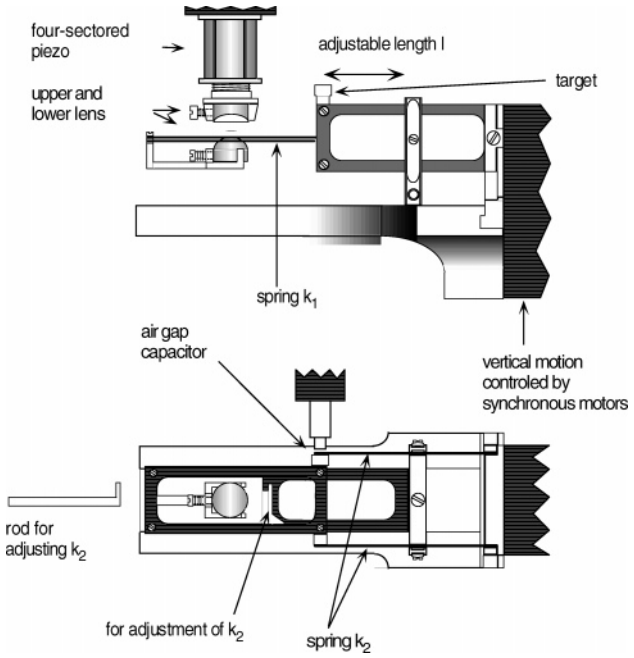

Figure 1. Schematic illustration of the new SFB design shown from the side and top view.

have the possibility to measure normal and lateral forces between two surfaces while monitoring their separation D independently. D is controlled by a three-stage mechanism: The coarse and intermediate mechanical control with a sensitivity 1 μm and 10 Å, respectively (not shown here), serve for positioning the surfaces to the desired range of distances. The finest control is achieved with a four-sectored piezo-electrical tube (PZT) to which the top surface is attached, allowing positioning and moving of the surfaces at the Å level. The sectored PZT further enables us to apply oscillating or steady shear motion with amplitudes up to a few μm, while D can be held constant to within a few Å using a feedback approach with the sectored PZT.[3,33] D is measured optically using multiple-beam interference fringes called fringes of equal chromatic order, or FECO.

The sectored piezo is detached from the shear-measuring spring κ_2. Thus normal and shear forces, when present, are sensed with the lower surface that is attached to the measuring horizontal (κ_1) and vertical (κ_2) double-cantilever springs. Shear is induced by moving the top surface laterally. In this design, the applicable shear frequencies are in principle only limited by the resonance frequency of the piezo $\omega_P \approx 120$ kHz. Here we present shear swelling results obtained for shear frequencies of 1 kHz.

Normal forces $F_\perp(D)$ are measured by expanding or contracting the piezo by a known distance ΔD_0, and simultaneously measuring optically the change in surface separation ΔD. Thus the normal force−distance profile is given by $F_\perp(D) = F(D + \Delta D) - \kappa_1(\Delta D_0 - \Delta D)$; $\kappa_1 \approx 70$ Nm^{-1}, and the sensitivity is about ± 0.1 μN.

Shear forces at a given distance $F_{||}(D)$ are measured with the vertical double-cantilever spring to which a small flat metal plate is attached. This plate faces a flat probe surface, forming a sensitive air-gap capacitor (Accumeasure 5000, MTI Instruments). If the lower surface experiences a shear force induced by the moving top surface, the shear spring κ_2 will be deflected, causing a change in the distance between plate and probe and thus changing the capacitance. This capacitance change can be translated into a bending amplitude $D_{||}$ and thereby to a shear force, $F_{||}(D) = -\kappa_2 D_{||}$. In contrast to the previous setup,[33] the stiffness of the shear-detecting spring can be varied during the experiment by shifting the position of the dovetailed clamp using the adjusting rod (Figure 1). In the weakest spring configuration, the full length of the spring l is free to move with a resonance frequency of about 60 Hz. The stiffness of a double-cantilever spring scales with its length as $\kappa_2 \sim l^{-3}$, thus we can adjust the stiffness to the desired values. Note that, during the high-frequency shear swelling measurements, we stiffened the shear-detecting spring in order to avoid resonances in the spring.

Here we focus on the coupling between shear and normal forces. These measurements are performed as follows: In the absence of shear motion, the surfaces are brought to a distance D. Then shear of a given frequency and amplitude is switched on. At high shear rates, a sudden change ΔD in the surface separation is observed. This change can be interpreted as an additional normal force $\Delta F_\perp = -\kappa_1 \Delta D$ due to the shear-induced swelling of the brushes (the sign of $\Delta F_\perp$ is defined to be positive for repulsion and negative for attraction). Throughout the present work, we denote $\Delta F_\perp$ as ΔF. When the shear is switched off, the surfaces relax back to their original separation D. This type of coupling is found to be specific to the experiments presented here and will be described in detail later. Two types of plots can be constructed: (1) Force ΔF versus distance D profiles, where the shear velocity is kept constant and only the separation is varied. (2) ΔF is monitored as function of shear velocity, v_s, at fixed separation. The velocity in these experiments is varied by changing the shear amplitude, while the frequency stays constant (it is, however, also possible to vary the shear velocity by varying the frequency).

The methodology of the experiments is as follows: Freshly cleaved mica sheets, silvered on one side, serve as model surfaces. These are glued to two cylindrical lenses that are arranged in a cross-cylindrical geometry. Prior to exposing the surfaces to any solution, they are brought into contact in air. This procedure provides us with three important measures: (1) The cleanliness of the atomically smooth surfaces is tested (the air contact is adhesive, thus van der Waals attraction should be experienced). (2) The contact position of the interference fringes in combination with the known wavelength of the spectral mercury lines serve as calibration of zero contact equivalent to a separation $D = 0$, relative to which other separations are subsequently measured. The surfaces are then separated, and a droplet of a PS−X/toluene solution of known concentration, ~0.1 mg/mL (around 10^{-6}−10^{-7} mol/L) is injected between them. After an hour of incubation, sufficient time for the polymer to form a dense brush as shown earlier,[32] normal force−distance and shear profiles are measured. In a final step, a filtered toluene solution of the free polymer, PS, at concentration 10 mg/mL, is injected into the already existing droplet of PS−X solution (Millipore Fluoropore filters, type FG, of pore size 0.2 μm are used). This procedure does not allow a precise control of the free polymer concentration. Furthermore, some evaporation of the solvent leads to a gradual increase of the polymer concentration. Therefore, in some experiments, we prepared the brushes outside the SFA after the calibration in air: The surfaces are immersed in a PS−X solution for 1 h then washed in toluene and dried with dry nitrogen. The dry brushes are mounted again into the SFA, and the PS solution is injected. A control experiment (not shown here) where pure toluene is injected between the dry brushes ensured that the brushes that have been prepared outside the cell relax back to a swollen configuration, exhibiting similar normal force/distance profiles. Equilibrium as well as shear-induced normal forces are then measured as described above.

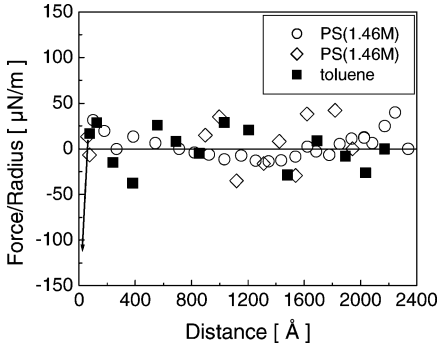

Figure 2. Normal interactions between bare mica surfaces in pure toluene and in the presence of PS (1.46 M) after an incubation time of 4 h (the polymer concentration is 10 mg/mL; two independent force-separation profiles are shown). The arrow indicates the jump into adhesive contact.

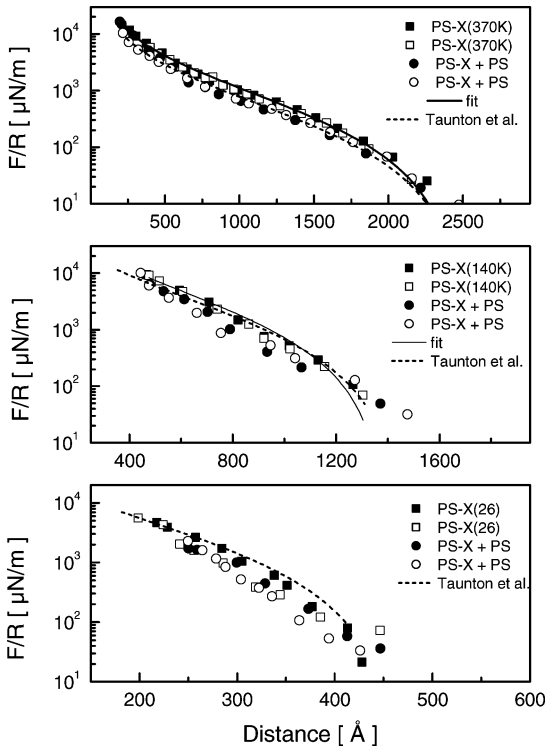

Figure 3. Normal force−distance profiles between PS−X (26K/140K/370K) brushes in toluene: measured by approaching (■) and receding (□) the surfaces. The solid line represents the best fit to these data using the Alexander−de Gennes expression[2,7,37] (eq 1) for the free energy between two brushes, and $2L_0$ as fitting parameter (see Table 1). The dashed lines are data by Taunton et al. obtained for the same brush lengths.[32] The force−distance curves measured in the presence of free PS chains are denoted by the circles (●, ○).

3. Results

3.1. Control Experiments for Nonadsorption of Unfunctionalized Polymer. Earlier experiments showed no adsorption of unfunctionalized polystyrene to mica from toluene.[32,34] Our control experiments, too (Figure 2), show no adsorption of free PS despite the high concentrations used here: $\Phi_f^b \approx 10^{-2}$, approximately 40 times greater than the overlap value Φ^* (see Table 1).

3.2. Normal Forces between PS Brushes with and without Added Free Polymer. In Figure 3, we show normal force profiles for three different brush lengths, PS−X (26K/140K/370K), measured both in pure toluene and in the presence of the semidilute solution of long free PS. The force profiles are normalized as (F/R), where R is the mean radius of curvature of the surfaces, which in the Derjaguin approximation[1] (valid here) corresponds to $2\pi E(D)$, where $E(D)$ is the corresponding interaction energy per unit area between flat parallel plates obeying the same force−distance law. The overall repulsive forces demonstrate that any depletion attraction caused by nonadsorbing polymer in solution is smaller than our detection limit, in line with estimates made earlier.[34,35] In the absence of free polymer, compression (approaching surfaces) and decompression (receding surfaces) profiles are measured and then fitted using eq 1. These profiles compare well with earlier measurements[32] of the same system (also shown in Figure 3), confirming the integrity of our experiments. Force profiles taken in the presence of free polymer ($\Phi_f^b \approx 10^{-2}$) show no alteration of the onset of repulsive interactions between the opposing brushes. At intermediate compressions, $1 > D/2L_0 >$ ca. 0.4, however, the measured normal forces are generally *systematically* lower by up to 30%, while at high compressions, $D/2L_0 < 0.3-0.4$, the force profiles both in the absence and presence of free polymer overlap again. This behavior is observed in all experiments.

3.3. Coupling between Shear and Normal Forces. Earlier experiments[3] on PS−X (140K) polymer brushes in toluene showed there is no coupling between normal and shear forces when the brush-bearing surfaces slide past each other at sufficiently low velocity v_s. However, above a critical value, $v_s > v_c$, a sudden stretching of the brushes was observed. This behavior is referred to as *brush swelling*. Here we present new experimental data on the same PS−X polymer brush system but extend it to two further polymer brush lengths. In addition, first shear swelling measurements under the influence of free polymer in solution are reported. In the following, we present shear swelling data in pure toluene and compare these with previous results. Subsequently, the dependence of the shear behavior on the molecular weight of the brush polymer is investigated. And finally, the influence of free polymer in the overlap regime on the sheared brushes is studied.

a. Shear Coupling in Absence of Added Free Polymer. We start by focusing on the coupling between rapid shear and the normal forces between PS−X (140K) brushes in pure toluene, measured with the new SFB setup, and compare them with results obtained using an earlier design by Klein et al.[3] Figure 4 shows the additional normal force $\Delta F/R$ observed for shear velocities that are larger than a critical value v_c. We compare $\Delta F/R$ measured at two distances: at slight compression ($D \approx$ 820 Å, Figure 4b), shear swelling commences at a critical velocity $v_c \approx 460 \pm 40$ μm/s (triangles), similar to the previous measurements (circles and squares). However, at separations, $D \approx 2L_0 = 1400$ Å, where the brushes just start to touch each other, we obtain $v_c \approx 480 \pm 40$ μm/s (up triangles), a much smaller value than reported by Klein et al.[3] ($v_c \approx 1200 \pm 50$ μm/s; circles and squares in Figure 4a). We believe that this discrepancy may be due to the fact that in the new SFB, the drive for the shear motion is completely decoupled from the force measuring springs, providing a higher sensitivity.

To get a more general picture, we investigated the influence of the molecular weight and separation on the critical shear velocity. The results (all measured in pure toluene), shown in Figure 5, were obtained by applying always the same shear frequency $f = 1$ kHz. The change in the shear velocity v_s was achieved by increasing the shear amplitude. For all three brush lengths, we see a dependence of the critical shear velocity on the separation (see also Figure 7). For a better comparison of this dependence, we plot the critical velocity as a function of the inverse compression $\beta^{-1} = D/2L_0$ (Figure 6). In all three

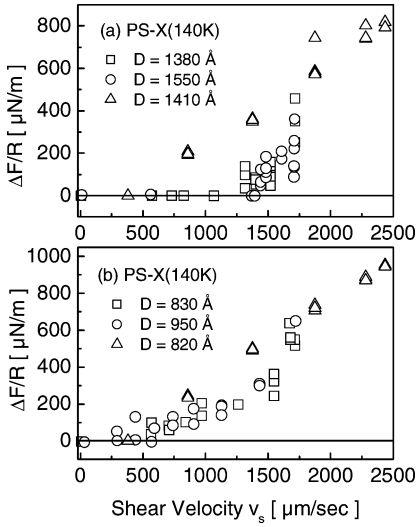

Figure 4. PS−X (140K) brushes in toluene (no free PS) under shear: variation of $\Delta F/R$ at fixed distances as a function of the shear velocity, v_s. The profiles are measured at separations corresponding to just overlap between the brushes ($2L_0 \approx 1400$ Å) (a), and at moderate compressions (b). In all measurements obtained with the new SFB (Δ), the applied lateral motion was sinusoidal with frequency $\nu = 1$ kHz, while the shear amplitude, Δx, was varied between 500 and 12 000 Å. The mean velocity is evaluated as $v_s = 2\nu\Delta x$. Data by Klein et al.[3] were obtained for shear frequencies $\nu = 400$ Hz and $\nu = 500$ Hz (□ and ○, respectively).

systems, a minimum in v_c is observed when the two brush layers just overlap, whereas for lower and higher compressions, v_c increases.

The dependence of $\Delta F/R$ as a function of the separation at fixed shear velocities v_s is presented in Figure 7: in the absence of free polymer, all three brushes PS−X (26K/140K/370K), show similar behavior. A coupling between shear and normal forces is observed at distances, $D > 2L_0$, which slowly grows as the surfaces are compressed until a maximum is reached at $D \leq 2L_0$. For even higher compressions, $\Delta F(D)$ decreases and eventually disappears. To ensure that this shear-induced normal force is indeed caused by the presence of the polymer brush and is not due to any instability of the apparatus, we measured $\Delta F/R$ also between *bare* mica surfaces in pure toluene for a similar value of v_s: the data in Figure 7c (crosses) indeed show, importantly, that no additional normal force occurs due to rapid shearing at all separations in the absence of a brush and free polymer.

b. Shear Coupling with Added Free Polymer. In the presence of free polymer, the picture changes dramatically. At distances larger than twice the equilibrium brush height, PS−X (26K) and PS−X (370K) brushes (Figure 7a,c) display no decrease in $\Delta F(D)$, which, however, persists and decays only slowly to zero at $D > 5000$ Å. Also the PS−X (140K) brushes show a different behavior, but $\Delta F(D > 2L_0)$ is now attractive. This attraction seems to be dependent on the concentration of the free polymer; at slightly higher concentration, this attraction disappears and only repulsion is experienced. For separations, $D < 2L_0$, the behavior of $\Delta F(D)$ for all three brush lengths is similar to the polymer-free case. Note also that, while the data is consistent, there is on occasion considerable scatter; thus in Figure 7b, the data indicated by solid and empty stars, while qualitatively similar (both data sets show a maximum followed by an attractive regime), differ quantitatively by a factor of almost 2, even though the shear velocities differ by only some 5%.

Figure 8 shows the critical shear rate versus the separation for PS−X (140/370) brushes with and without free PS-chains

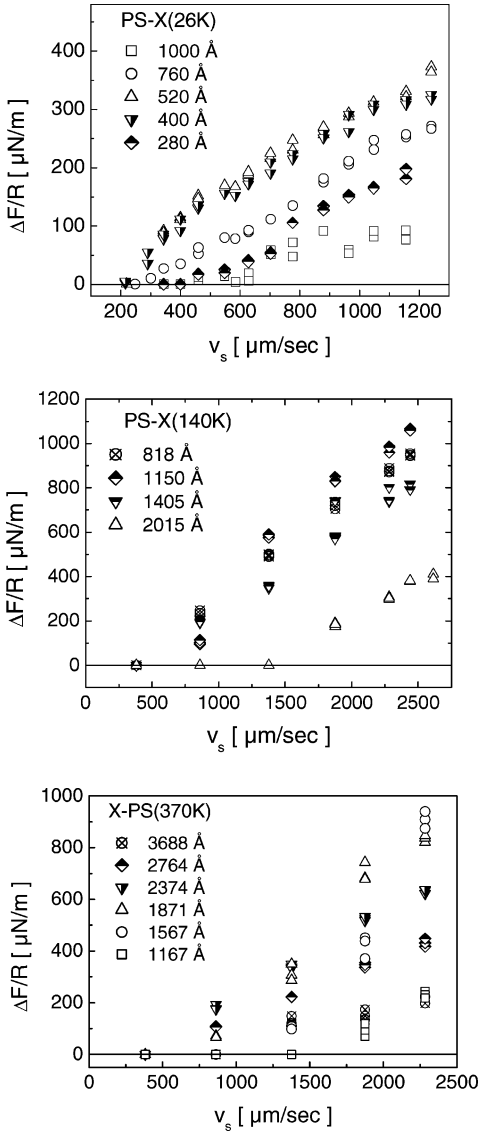

Figure 5. $\Delta F/R$ vs shear velocity v_s for PS−X (26K, $2L_0 \approx 430$ Å), PS−X (140K, $2L_0 \approx 1400$ Å), and PS−X (370K, $2L_0 \approx 2400$ Å) brushes measured in pure toluene. Profiles are presented for various separations: At larger distances $D > 2L_0$, when the opposing brushes just overlap $D \approx 2L_0$, and at moderate compressions, $D < 2L_0$. In all cases, we fixed the shearing frequency to 1 kHz while the amplitude was varied.

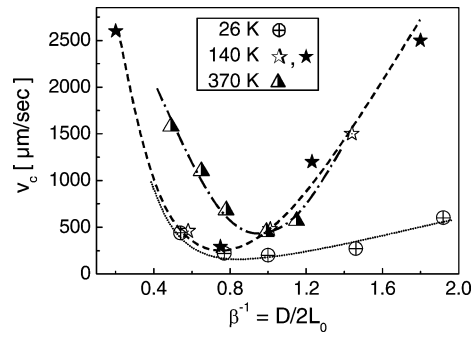

Figure 6. Critical shear velocities v_c as a function of compression $\beta^{-1} = D/2L_0$ for three different brush lengths. Earlier measurements by Klein et al.[3] for PS−X (140K) are indicated by the ★ symbol. The lines are guides to the eye.

(Figure 8b,c) and for PS−X (26K) in pure toluene (Figure 8a). We define the effective critical shear rate, $\dot{\gamma}_c$, between two brush-covered surfaces as follows: In the nonoverlapping

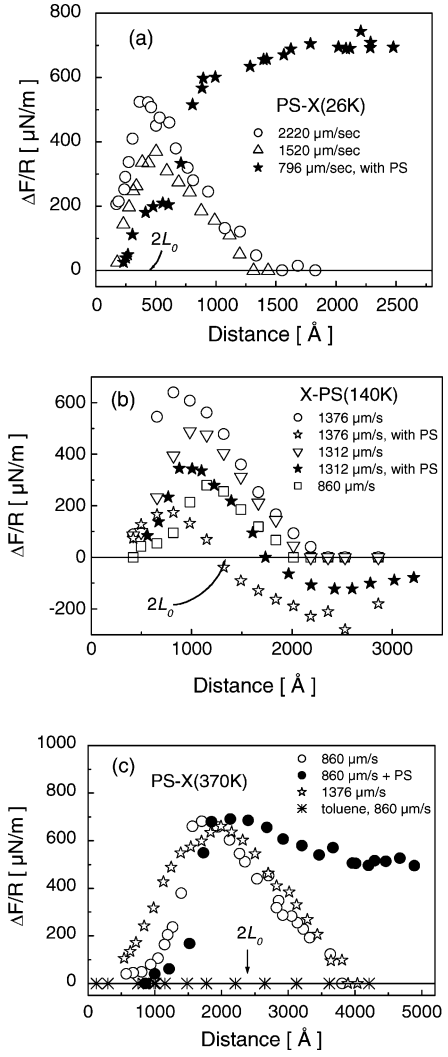

Figure 7. $\Delta F/R$ measured as function of separation D, at different shear velocities, v_s, for (a) PS−X (26K), (b) PS−X (140K), and (c) PS−X (370K) brushes.

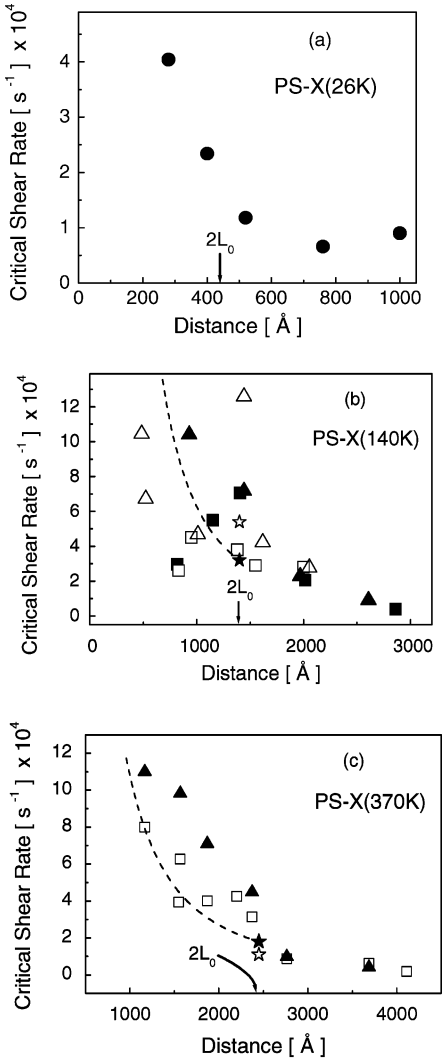

Figure 8. Effective critical shear rate $\dot{\gamma}_c(D)$ (defined in the text) as a function of the surface separation measured for the three different brush lengths. (a) PS−X (26K) brushes: $\dot{\gamma}_c(D)$ measured in pure toluene. (b) PS−X (140K) brushes: Data obtained with the new SFB (■) and by Klein et al.[3] (□) in the absence of free PS. $\dot{\gamma}_c(D)$measured in the presence of free PS are represented by △ and ▲, obtained from two different experiments. The empty star is the evaluated Zimm relaxation rate τ_z^{-1} (ξ) from Table 2, and the solid star is the estimated mean value of the effective critical shear rate at $D = 2L_0$. The curve (starting at the solid star) corresponds to the variation $\dot{\gamma}_c(D) \sim D^{-9/4}$. (c) PS−X (370K) brushes: Empty squares (□) and filled triangles (▲) are for measurements in pure toluene and in the presence of free PS, respectively. The empty star (☆) is the evaluated Zimm relaxation rate $\tau_z^{-1}(\xi)$ from Table 2, and the solid star (★) is the estimated mean value of the effective critical shear rate at $D = 2L_0$. The curve (starting at the solid star) corresponds to the variation $\dot{\gamma}_c(D) \sim D^{-9/4}$.

region, $D > 2L_0$, $\dot{\gamma}_c$ may be estimated as $\dot{\gamma}_c = v_c/(p + 2\delta_H)$, where p is the gap between the brush ends and δ_H the hydrodynamic penetration of the fluid flow into the brush as suggested by Klein.[2] Earlier lubrication force studies[36] show that the penetration depth of a simple Newtonian liquid flowing past a brush is at most of the order of the correlation length or blob size, thus $\delta_H \approx \xi$. Under compression, $D < 2L_0$, we expect shear stress to be experienced only in the zone of mutual interpenetration d of the two brushes. This is predicted[2] to scale as $d(D) = s(2L_0/D)^{1/3} = s\beta^{1/3}$, where the mean interanchor spacing s is roughly equal to the blob size ξ. The effective critical shear rate for $D < 2L_0$ can thus be estimated as $\dot{\gamma}_c = v_c/d$. Note that, at $D = 2L_0$, $d = s \approx \xi$, while $p = 0$, so that the two estimates of the effective critical shear rate $\dot{\gamma}_c$ are equal within a factor of order two for $D = 2L_0$. Data by Klein et al.[3] on PS−X (140K), indicated in Figure 8b, are in reasonably good agreement with the present experimental results. In Figure 8, too, as in Figure 7, there is substantial scatter in the data, which may originate from the presence of small local inhomegeneities in the structure of the brush at different points on the surface and reflects the sensitivity of the critical shear rate to such structure. The overall picture one obtains for the three brush lengths is that the effective critical shear rate increases with increasing compression of the brushes. This is discussed more quantitatively in the following section.

4. Discussion

4.1. Effect of Free Polymers on the Equilibrium Brush Height. The main investigation of this study involved measuring the change in normal forces between two opposing polymer brushes undergoing shear with respect to each other. This shear-induced change was measured as a function of shear-velocity/shear-rate at different surface separations. We extended an earlier preliminary study[3] of this type of interaction and, in particular, for the first time investigated the effect of added free polymer. In this section, we discuss both similarities and differences for the two types of configuration (i.e., with and without added free polymer).

The normal force profiles between two brush layers in a good solvent measured with the more recent SFB design show good

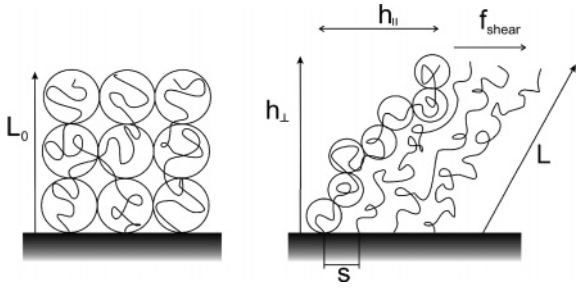

Figure 9. Illustration of the unperturbed (left) and sheared brush (right).

agreement with results obtained by Taunton et al.[32] Pioneering theoretical work on end-anchored, nonadsorbing chains was done by Alexander and de Gennes:[7,37] Each grafted polymer chain can be pictured as string of blobs, as shown in Figure 9, thus forming a brush-layer consisting of semidilute blobs. The thickness of the brush scales as $L_0 \approx Ns^{-2/3}a^{5/3}$, and a scaling expression for the interaction force per unit area $f(D)$ between two parallel plates bearing such brush layers was developed by de Gennes:[7]

$$f(D) \approx (k_B T/s^3)[(2L_0/D)^{9/4} - (D/2L_0)^{3/4}], \quad \text{for } D \leq 2L_0 \quad (1)$$

Here k_B and T are Boltzmann's constant and the temperature, respectively. The first term in square brackets stems from the osmotic repulsion experienced by the brushes, as they are compressed. The reduction in the free energy due to the compression of the overstretched chains is expressed in the second term. Equation 1 was used to fit the normal force profiles in Figure 3. This model assumes that the monomer distribution away from the surface is steplike. However, subsequent theories based on self-consistent mean-field calculations[38−40] show that the distribution of the monomer concentration within the brush is parabolic. This implies that the blob diameter or correlation length increases with the distance from the solid surface.[12,34] The blob size in the outmost layer reflects the scale over which the brush−solvent interface is smeared out. Thus the free polymer chains, when present, will face a more dilute monomer concentration at the outer fringe of the brush. This is equivalent to having a diffuse rather than a sharp interface. Consequently, some penetration of the PS chains into the brush is possible. Nevertheless, the Alexander model proves to give a good estimate of the equilibrium brush height L_0 under good solvent condition and in the absence of free polymer.

Scaling arguments by de Gennes[7] as well as mean-field calculations by Wijmans et al.[26] predict shrinkage of the brush height in the presence of free polymer with identical chemical nature as the brush polymer. This shrinkage and a possible penetration of the free polymer into the brush will strongly depend on the grafting density σ, the degree of polymerization of the brush and the free polymer N_g and N_f, respectively, and in particular on the volume fraction of the free polymer in the bulk Φ_f^b. Wijmans et al. distinguish various scaling regimes and predict for high grafting densities a change in the scaling dependence of L from that of a strongly stretched brush ($L \sim N_g$) to that of a Gaussian coil ($L \sim N_g^{1/2}$).

Qualitatively, this is because one would expect shrinkage of the brush height when the volume fraction of the free polymer exceeds that of the brush Φ_g. In this case, the osmotic pressure of the solution compresses the brush and only little penetration of the free chains occurs. In the present experiments, the volume fraction of the free PS-chains, Φ_f^b, was well above the mean overlap concentration c^* (Table 1: $\Phi_f^* \approx 2.7 \times 10^{-4}$), but still below the mean monomer concentration within the brush (we estimate an average $\Phi_{140K} \approx 4 \times 10^{-2}$, and Φ_{370K} to be lower by a factor of 2, assuming a steplike profile of Φ_g). And indeed, no marked change in the onset of interaction was found within the scatter (Figure 3). However, for compressions down to $\beta^{-1} \approx 0.25$, the value of the normal interactions is as much as 20−30% lower in the presence of free polymer for all brush lengths. At even higher compressions, the force profiles with and without free PS in solution overlap again. How are we to explain this? A possible qualitative explanation is as follows: As noted earlier, the monomer distribution within the brush is not steplike but of parabolic shape, leaving us with a more dilute monomer concentration at the brush−free polymer interface. Thus the (free) monomer concentration within the bulk solution may exceed that of the outer part of the brush and so lead to its compression. At the same time, free polymer will be entangled with the outer blob of the brush, and so be weakly "trapped" between the brushes (such trapping effectively eliminates any depletion attraction effects[35]). As the surfaces approach, initial repulsion between them may occur as a result of the osmotic pressure due to this weakly "trapped" free polymer. This effect will be transient but may be sufficient to result in the effective onset of repulsion being similar (within the experimental scatter) to that of the more swollen brushes in the absence of free polymer. As the surfaces approach further, the increased pressure is sufficient to squeeze out the excess free polymer from within the gap: the result of this removal of free polymer from the gap on compression is that the repulsion is weaker than it would have been if only fixed brush chains were being compressed. This explains, qualitatively, the 20−30% weaker repulsion in the intermediate compression regime observed for brushes + free polymer, compared to brushes alone, in the profiles of Figure 3. Finally, at the highest compressions, all free polymers will have been squeezed out and further compression merely results in the increased osmotic repulsion expected from brushes alone. We indeed observe in Figure 3 that, at the highest compressions, the force profiles of both the polymer-free and added polymer brushes converge.

To summarize, all three brushes show little change in the range of the force−distance profiles in the presence of free, overlapping PS chains. This may be due to a combination of some shrinkage of the outer part of the brushes together with additional repulsion due to free polymer in the gap between the brushes resulting from free polymer weakly trapped by entanglement with the brushes. In this context, experimental results by Lee et al.[25] should be mentioned, which do indicate a strong shrinkage of the brush at $\Phi_f^b \approx 10^{-1}$, an order of magnitude greater than the concentration we used. Our assumption that we have some entanglement coupling between the free polymer and the brush-covered surfaces is supported by the shear results that we discuss in the following paragraph.

4.2. High Shear Rates: Shear Swelling. The Alexander−de Gennes theory assumes a steplike profile of the monomer distribution within the brush.[7,37] Thus assumption is sufficient to describe the equilibrium state of the brush but does not address shear-induced swelling of brushes. A first model addressing this effect was proposed by Rabin and Alexander.[14] Their main finding is that, when a polymer is subject to a shear flow of a simple Newtonian liquid, the chains, described by a string of blobs, will tilt but the overall thickness will stay unaffected. A reinterpretation of these results by Barrat,[41] on the other hand, predicts a maximum 25% increase in L when the brushes experience a shear flow. A simple way of understanding his argument is as follows: The unperturbed brushes form a close packed array of blobs, where the stretching

Table 2

sample	ξ, Å	$v_s(2L_0)$, μm/s	$\dot{\gamma}_c$, s^{-1}	$\tau_Z(\xi)^{-1}$, s^{-1}
PS−X (26K)	47	250 ± 50	$(2.8 \pm 0.5) \times 10^4$	3.2×10^5
PS−X (140K)	85	480 ± 50	$(3^{+2}_{-1}) \times 10^4$	5.4×10^4
PS−X (370K)	143	520 ± 50	$(1.8 \pm 0.9) \times 10^4$	1.1×10^4
PS (1.46 M)	81[a]			6.5×10^4

[a] ξ (1.46 M) is taken to be the correlation length in a semidilute solution: $\xi = R_F(\Phi^*/\Phi)^{3/4}$, where $\Phi = 40 \times \Phi^*$. The Zimm relaxation rate is evaluated using the relation $\tau_Z(\xi)^{-1} = k_BT/4\pi^3\eta_s\xi^3$, and the critical shear rate $\dot{\gamma}_c$ is estimated at $D = 2L_0$ as $\dot{\gamma}_c = v_s(2L_0)/2\xi$ as described in the text.

and the osmotic pressure are in equilibrium. On shearing and extending the chains laterally, each chain breaks up into a larger number of smaller blobs, as illustrated in Figure 9. This implies that the osmotic pressure within the brush that arises from the blob−blob interactions increases. In other words, the shear stretching reduces the screening of the osmotic interactions within the brush. Therefore, the already-swollen brush will be swollen even further, leading to an additional normal force $\Delta F(D)$, which ceases as the shear stress is switched off. A theoretical study by Harden and Cates,[12] who propose a nonuniform stretching of the chains in the flow field, comes to similar conclusions, while Kumaran[13] predicts a stretching of the brush chains up to 33% using hydrodynamic arguments.

Experiments by Klein et al.[3] as well as our data (Figures 4−8) suggest that an additional swelling of brushes in pure solvent indeed occurs when high enough shear flows are applied. However, the theories mentioned above do not predict the shear velocity at which shear swelling may be expected and how this critical value is dependent on the molecular weight and hence the blob size. As pointed out, shear-induced swelling in pure solvent only occurs above a critical shear velocity, $v_s > v_c$, which varies with the brush and with D. This suggests that the outer layer of the brush chains will stretch only when the fluid shear rate $\dot{\gamma}_c$ is higher than the corresponding relaxation rate τ^{-1} of the outer brush moieties being sheared. Harden and Cates[12] propose to relate τ^{-1} to the relaxation rate $\tau_Z(\xi)^{-1}$ of a non-free-draining blob of size ξ (its Zimm relaxation rate). This may be estimated as $\tau_Z(\xi)^{-1} \approx k_BT/4\pi^3\eta_s\xi^3$, the characteristic rotational diffusion rate of a sphere of hydrodynamic diameter ξ in a liquid of viscosity η_s. Thus we propose that shear swelling occurs when $\dot{\gamma} > \dot{\gamma}_c = \tau_Z(\xi)^{-1}$, where $\dot{\gamma}_c$ is the effective critical shear rate. We defined $\dot{\gamma}_{max}$ earlier for the different surface separation regimes as $\dot{\gamma}_c = v_c/(p + 2\delta_H)$, where p is the gap between the brush ends and δ_H ($\approx \xi$) the hydrodynamic penetration of the fluid flow into the brush for the regime $D > 2L_0$ and as $\dot{\gamma}_c = v_c/d$ (where $d(D) = s(2L_0/D)^{1/3} = s\beta^{1/3}$, $s \approx \xi$) for $D < 2L_0$. These are clearly only estimates because the brush edge is not a sharp boundary, nor is the penetration depth well-defined as ξ, and, especially in the regime $D \approx 2L_0$, these expressions are likely to result in a significant scatter for the value of $\dot{\gamma}_c$, as is indeed seen in Figure 8. Nonetheless, these expressions provide at least a consistent semiquantitative estimate for $\dot{\gamma}_c$, and it is of value to use them to examine the molecular models for brush shear. In Table 2, we compare the calculated Zimm rates and the experimental values for $\dot{\gamma}_c$ estimated (from the above expressions) using the experimentally obtained critical shear velocities v_c at $D \approx 2L_0$. The experimental values of $\dot{\gamma}_c(D)$ as a function of D are plotted in Figure 8, and a comparison of these two values (the calculated values from Table 2 are shown as empty stars in Figure 8b,c) shows that the interpretation of $\tau_Z(\xi)^{-1}$ as a threshold, above which shear swelling is to be expected, is reasonable. Further we can see from Figure 8b,c and from Table 2 that, while the critical velocity increases with increasing blob size or molecular weight, the critical shear rate $\dot{\gamma}_c$ and the relaxation rate $\tau_Z(\xi)^{-1}$ both decrease (see later discussion why this may not apply well to the 26K brush, Figure 8a). This latter result, while counterintuitive, is indeed qualitatively in line with our expectations that the critical shear rate tracks the Zimm relaxation rates of the outer blobs on the brushes.

Further support for this concept is provided by examining in more detail the $\dot{\gamma}_c(D)$ variation in Figure 8. For the separation regime $D > 2L_0$, we expect the value of ξ to remain constant (because the brushes are uncompressed) so that $\tau_Z(\xi)^{-1}$ is essentially constant and we expect little change in $\dot{\gamma}_c(D)$ with increasing D. This is indeed the trend seen for all three brushes at $D > 2L_0$. For $D < 2L_0$, however, we expect that, as the brushes compress, the blob size decreases as $\xi \sim \phi^{-3/4}$ (e.g., ref 42), where the monomer volume fraction ϕ within the brush increases as $\phi \sim D^{-1}$. Thus if the effective critical shear rate tracks the Zimm relaxation rate $\tau_Z(\xi)^{-1} \approx k_BT/4\pi^3\eta_s\xi^3$, we would expect $\dot{\gamma}_c(D) \sim \xi^{-3} \sim D^{-9/4}$. This variation is shown as the dotted curve in Figures 8b,c and is indeed seen to represent the variation of $\dot{\gamma}_c(D)$ closely within the scatter. We conclude that both for $D > 2L_0$ and for $D < 2L_0$, the idea that swelling occurs at the point where the effective critical shear rate exceeds the Zimm relaxation rate of the (outer) blobs appears to describe the data quantitatively rather well, at least for the longer brushes.

It is appropriate to point out one limitation of this comparison. The main discrepancy to note, in Table 2, is that while for the 140K and 370K brushes, both the magnitude of $\dot{\gamma}_c(D)$ at $D = 2L_0$ and its variation with D (as in Figure 8b,c) are, within the scatter, in line with those expected based on the Zimm relaxation rate, this is not the case for the 26K brush. For this shortest brush (Table 2), the effective critical shear rate $\dot{\gamma}_c(D = 2L_0)$ is about an order of magnitude lower than the predicted Zimm relaxation rate. There may be a number of reasons for this: the main one, we believe, is that in the case of the 26K brush, the scaling assumptions for the blob size may not hold as well as they do for the longer brushes. Thus if we take each chain of the brush to have some 8 blobs (as suggested in ref 32), each blob would consist of only some 30 styrene monomers, barely a statistical step length. Independent indications that this shortest PS−X brush does not follow the scaling trend of the longer ones were seen already in the earlier comprehensive work on PS−X brushes[32] (as well as in our present study, which reproduces the profiles of that paper): the mean interanchor spacing s for the 26K differed significantly from the value expected based on the scaling trend of the longer brushes in that study.[32] Moreover, while for all longer brushes studied,[32] the ratio of brush height to the corresponding mean interanchor spacing (i.e., L_0/s) was some 7-to-8-fold or more, for the case of the 26K brush, this ratio was only 4.5-fold. This anomalous behavior may imply that the ideas advanced for the longer brushes, while qualitatively correct also for the shorter brush, may apply less well quantitatively. Thus a 2-fold error in our estimate of the size ξ of the outer blob of the 26K brush would result in a $2^3 = 8$-fold error in the predicted critical shear rate, which would largely explain the discrepancy in Table 2. We thus have more confidence in the quantitative comparison of the model with the longer (140K and 370K) brushes, and it is therefore with the results for these brushes that quantitative comparisons are made.

To understand the coupling of normal and shear forces at distances (Figure 7) where swelling is not observable in the absence of free polymer, we refer to Figure 10: we assume that the free polymer penetrates the brush−solvent interface and thus forms a semidilute polymer network from one surface to

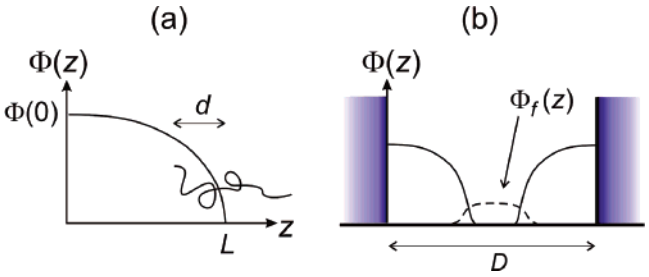

Figure 10. (a) Schematic illustration of the parabolic monomer density profile $\Phi(z)$ of a brush of thickness L; d is the penetration depth of an opposing brush. (b) Simplified sketch of a possible distribution of the monomer density of the two brushes Φ_g and the free polymer Φ_f^b in between them.

the other. In the case of added free polymer, this network transmits the shear motion of the top to the lower surface even when they are far apart. Both PS−X (26.5K/370K) show (Figure 7) a repulsive $\Delta F(D)$ at large D ($\gg L_0$) due to shear swelling, whereas attraction is seen in the PS−X (140K)/PS system. We do not have an unambiguous explanation for this. However, it is suggestive that, as shown in Table 2, the blob size in the Alexander model for the PS−X (140K) brush and the correlation length ξ for the free polymer at 1% concentration are very similar as are, therefore, their Zimm relaxation rates. From simple considerations, one would then expect the dynamic coupling between the free polymer in the gap and the brush outer layer to be optimal for the PS−X (140K) brushes: when the shear rate exceeds the critical value for swelling of these brushes, it will also stretch the free polymer network. This would result in a lateral restoring force between the surfaces, due to the stretched network, with a component in the normal direction tending to attract them via the entanglement of the free chains with the brush. Such an effect might explain the attraction observed between the PS−X (140K) brushes at high shear rates in the presence of free polymer (Figure 7B). In the case of both of the other two brushes, the dynamic coupling is expected to be less favorable (due to the mismatch in correlation lengths and relaxation rates), and the network of free chains in the gap would not undergo such lateral stretching. Thus, as observed, only repulsion due to brush swelling will occur. It is of interest that this attraction in the case of the PS−X (140K) brushes seems to be dependent on the volume fraction of the free polymer. We observed (not shown here) that the attraction turns into repulsion as the drop (between the surfaces) becomes smaller so that the effective concentration of free polymer increases. This would be in line with the explanation given above because, at significantly higher free polymer concentration, its correlation length would no longer match that of the blob size in the brush.

One important question we have not yet addressed is why we observe what appears to be shear-induced brush swelling when two opposing brush layers are sheared (in an oscillatory fashion), in line with several theoretical and simulation studies,[11−13,15,41] while neutron-reflectivity experiments[16,17] and some theories[14] and simulations[20] on a sheared single brush do not indicate such an increase in layer thickness. Because the simulations have clear limitations (recognized in the papers themselves[18,22,23]), we consider here in particular the neutron reflectometry studies,[16,17] which show no brush swelling and have been taken to contradict the earlier study[3] (and by implication also the present results, which reproduce the earlier work), which does purport to show brush swelling at high enough shear rates. In the study of ref 17, a physisorbed diblock PEO-PS copolymer (used also in ref 32) is attached by its adsorbing PEO moiety onto quartz to form a brush whose monomer volume fraction ranges from 5% to zero. Under shear rates up to 1×10^4 s^{-1}, there is no significant change in the reflectivity profile relative to zero shear, while at a shear rate 2×10^4 s^{-1}, some 50% of the brush appears to desorb.[45] Two comments are in order: First, it would appear that the sensitivity of neutron reflectometry is insufficient to detect a small swelling (up to 25% increase L_0) of the brush above the noise level in the reflectometry data. This limitation was deduced by simulating the brush−substrate system in detail[43] and is supported by the fact that even following a 50% or so loss of polymer upon desorption (Figure 3 of ref 17), the difference in the reflectometry profile to that of the undesorbed chain is barely above the scatter in the data. There is, however, an additional point that makes the results of this study[17] unsuitable for comparison with the shear swelling reported here and in ref 3: That is that the maximal shear rate, $\dot{\gamma}_{\max(17)}$, attained in ref 17 is either below the level required to shear-swell the brush layer in that study, or at a level where the polymer begins to desorb. This is readily seen by evaluating the mean interanchor spacing[44] for the copolymer brush in ref 17, which yields a value somewhat larger than that of the 140K brush in the present study, 101 Å versus 84 Å. This implies, from the earlier discussion and the data in Figure 8b and Table 2 for the effective critical shear rate of the 140K brush, that a shear rate, $\dot{\gamma}_c \approx (84/101)^3 \times (3 \times 10^4)$ s^{-1} $\approx 1.7 \times 10^4$ s^{-1}, would be necessary to stretch and swell the diblock brushes used in ref 17. Because in fact the highest shear rate $\dot{\gamma}_{\max(17)} = 1 \times 10^4$ s^{-1} actually reported (prior to polymer desorption) is lower than this, and because at higher values in that study ($(1-2) \times 10^4$ s^{-1}) polymer desorption occurs, one would not expect any shear-induced swelling, quite apart from the question of sensitivity noted above. Thus the results of this neutron reflectometry study[17] do not contradict the current and the earlier[3] observations of swelling at sufficiently high shear rates.

In the other neutron reflectometry study,[16] PS chains ($M =$ 80K) were chemically grafted to a silicon block (so that desorption under shear is suppressed) and shear rates up to a value $\dot{\gamma}_{\max(16)} = 1.3 \times 10^5$ were observed not to result in any swelling of the brushes. The grafting densities used were high, with a mean interanchor spacing $s = 28$ Å, and the mean brush densities were also high, with polymer volume fractions in the brush layers ranging from 25% (in toluene) to 50% (in cyclohexane), so that, unlike the case of ref 17, the reflectometry profiles should certainly detect even small variations in brush height. We may assume that the shear rate required to swell the brush layers (PS 80K/toluene) in this study[16] corresponds to the corresponding inverse Zimm relaxation rate, a relation that holds well for the 140K and 370K brushes (Table 2 and Figure 8a,b). Then, setting as before $s \approx \xi$ and substituting in the expression for $\tau_Z(\xi)^{-1}$, we estimate that the required shear rate for stretching the outer blobs of these brushes is $\dot{\gamma}_c \approx 7.5 \times 10^5$ s^{-1}: this is some 6-fold higher than the rate $\dot{\gamma}_{\max(16)} = 1.3 \times 10^5$ actually achieved in ref 16. Thus we may conclude that the nonobservance of shear swelling in that study[16] is the result of applying an insufficiently high shear rate. The overall conclusion from the above analyses is that in neither of these neutron reflectivity studies[16,17] was a sufficiently high shear rate applied to induce swelling in the brushes, and so neither study is in contradiction to the shear swelling observations of ref 3 and of the present study.

To summarize, normal forces between two surfaces bearing dense brushes in the absence and presence of mobile polymer chains were measured as a function of their separation and shear

velocities. The results confirm and extend those of an earlier study,[3] and could be quantitatively interpreted in terms of a shear-induced swelling picture where the critical shear rate for inducing the swelling is comparable to the Zimm relaxation times of the outer blobs on the brushes. The presence of the free polymer above the overlap concentration, c^*, did not alter the normal interactions significantly, although a reduction in the normal forces at intermediate compressions could be interpreted as a deswelling of the outer brush layers. The shear experiments, where high shear rates in lateral motion were applied, indicate that the mobile PS chains penetrate the outer layer of the brushes and a long-ranged coupling between normal and shear forces was observed, generally leading to repulsive interactions. This finding suggests there may be an entanglement coupling between the brush and the free polymer as proposed by Yerushalmi-Rozen and Klein[27] in their study of the effect of free polymer/brush combinations on wetting of solid surfaces.

Acknowledgment. We are especially appreciative of the help of Dr. R. K. Thomas in simulating the neutron reflectometry profiles of ref 17 (see also ref 43) and are grateful to Dr. L. J. Fetters for donation of the zwitterionic-terminated polystyrene molecules. We also appreciate constructive comments by the reviewers of this manuscript. We thank the EPSRC, the Petroleum Research Fund (grant 45964-AC7), the Charles McCutchen Foundation, and the Israel Science Foundation for support of this work.

References and Notes

(1) Klein, J.; Kumacheva, E.; Perahia, Mahalu, D.; Warburg, S. *Faraday Discuss.* **1994**, *98*, 173−188.
(2) Klein, J. *Annu. Rev. Mater. Sci.* **1996**, *26*, 581−612.
(3) Klein, J.; Perahia, D.; Warburg, S. *Nature* **1991**, *352*, 413−415.
(4) Grest, G. S. In *Polymers in Confined Environments*; Springer-Verlag: Berlin, 1999; Vol. 138, pp 149−183.
(5) Zhao, B.; Brittain, W. J. *Prog. Polym. Sci.* **2000**, *25*, 677−710.
(6) Halperin, A.; Tirrell, M.; Lodge, T. P. *Adv. Polym. Sci.* **1992**, *100*, 31.
(7) de Gennes, P. G. *Macromolecules* **1980**, *13*, 1069−1075.
(8) Milner, S. T. *Science* **1991**, *251*, 905.
(9) Klein, J.; Kumacheva, E.; Mahalu, D.; Perahia, D.; Fetters, L. J. *Nature* **1994**, *370*, 634.
(10) Raviv, J.; Giasson, S.; Kampf, N.; Govi, J. F.; Jerome, R.; Klein, J. *Nature* **2003**, *425*, 163−165.
(11) Aubouy, M.; Harden, J. L.; Cates, M. E. *J. Phys. II* **1996**, *6*, 969−984.
(12) Harden, J. L.; Cates, M. E. *Phys. Rev. E* **1996**, *53*, 3784.
(13) Kumaran, V. *Macromolecules* **1993**, *26*, 2426.
(14) Rabin, Y.; Alexander, S. *Europhys. Lett.* **1990**, *13*, 49−54.
(15) Doyle, P. S.; Shaqfeh, E. S. G.; Gast, A. P. *Phys. Rev. Lett.* **1997**, *78*, 1182−1185; *Macromolecules* **1998**, *31*, 5474−5486.
(16) Ivkov, R.; Butler, P. D.; Satija, S. K.; Fetters, L. J. *Langmuir* **2001**, *17*, 2999−3005.
(17) Baker, S. M.; Smith, G. S.; Anastassopoulos, D. L.; Toprakcioglu, C.; Vradis, A. A.; Bucknall, D. G. *Macromolecules* **2000**, *33*, 1120−1122 (following submission of our manuscript, an extension to different brush lengths of this reflectometry work by the same group has appeared: Anastassopoulos, D. L.; Spiliopoulos, N; Vradis, A.A.; Toprakcioglu, C.; Baker, S. M.; Menelle, A. *Macromolecules* **2006**, 39, 8901−8904).
(18) Wijmans, C. M.; Smit, B. *Macromolecules* **2002**, *35*, 7138−7148.
(19) Miao, L.; Guo, H.; Zuckermann, M. J. *Macromolecules* **1996**, *29*, 2289−2297.
(20) Grest, G. S. *Phys. Rev. Lett.* **1996**, *76*, 4979−4982.
(21) Lai, P.-Y.; Lai, C.-Y. *Phys. Rev. E* **1996**, *54*, 6958−6961.
(22) Saphiannikova, M. G.; Pryamitsyn, V. A.; Cosgrove, T. *Macromolecules* **1998**, *31*, 6662−6668.
(23) Saphiannikova, M.; Neelov, I.; Pryamitsyn, V.; Darinskii, A. A.; Sundholm, F. *Rheol. Acta* **2000**, *39*, 469−475.
(24) Auroy, P.; Auvray, L. *Macromoelcules* **1996**, *29*, 337−342.
(25) Lee, L. T.; Factor, B. J.; Rondelez, F.; Kent, M. S. *Faraday Discuss.* **1994**, *98*, 139−147.
(26) Wijmans, C. M.; Zhulina, E. B.; Fleer, G. J. *Macromolecules* **1994**, *27*, 3238−3248.
(27) Yerushalmi-Rozen, R.; Klein, J. *Langmuir* **1995**, *11*, 2806−2814.
(28) Safran, S. A.; Klein, J. *J. Phys. II* **1993**, *5*, 749−757.
(29) Sevick, E. M.; Williams, D. R. M. *Macromolecules* **1994**, *27*, 5285−5290.
(30) Raviv, U.; Tadmor, R.; Klein, J. *J. Phys. Chem. B* **2001**, *105*, 8125−8134.
(31) Eiser, E.; Klein, J.; Witten, T. A.; Fetters, L. J. *Phys. Rev. Lett.* **1999**, *82*, 5076−5079.
(32) Taunton, H. J.; Toprakcioglu, C.; Fetters, L. J.; Klein, J. *Macromolecules* **1990**, *23*, 571−579.
(33) Klein, J.; Kumacheva, E. *J. Chem. Phys.* **1998**, *108*, 6996−7009.
(34) Luckham, P. F.; Klein, J. *Macromolecules* **1985**, *18*, 721−728.
(35) Ruths, M.; Yoshizawa, H.; Fetters, L. J.; Israelachvili, J. N. *Macromolecules* **1996**, *29*, 7193−7203.
(36) Klein, J.; Kamiyama, Y.; Yoshizawa, H.; Israelachvili, J. N.; Fredrickson, G. H.; Pincus, P.; Fetters, L. J. *Macromolecules* **1993**, *26*, 5552−5560.
(37) Alexander, S. *J. Phys. France* **1977**, *47*, 1243.
(38) Milner, S. T.; Witten, T. A.; Cates, M. E. *Macromolecules* **1988**, *21*, 2610.
(39) Zhulina, E. B.; Priamitsyn, V. A.; Borisov, O. V. *Vysokomol. Soedin. A* **1989**, *31*, 1615.
(40) Milner, S. T. *Macromolecules* **1991**, *24*, 3704−3705.
(41) Barrat, J.-L. *Macromolecules* **1992**, *25*, 832 - 834.
(42) De, Gennes, P.G. *Scaling Concepts in Polymer Physics*; Cornell University Press, Ithaca, NY, 1979
(43) Thomas, R.K. private communication based on quantitative evaluation of reflectometry profiles corresponding to conditions of ref 17.
(44) The mean interanchor spacing s for the PEO−PS (184K) brush in ref 17, where the PS tail has $M = 170$K, may be evaluated by estimating the adsorbance of the polymer from the inset to Figure 3 in that work to yield a value of 2.8 mg/m^2, corresponding to $s \approx 101$ Å.
(45) Desorption under shear of the PS−PEO brushes in ref 17, anchored by an adsorbing PEO moiety, is expected to be much easier than for the PS−X chains anchored by a zwitterion used in the present study. This is because "unzipping" of the adsorbed PEO by shear need only overcome the relatively weak single-PEO segment/substrate adhesion energy (of order 0.1 k_BT) compared with overcoming the 7−8 k_BT energy associated with adhesion of the zwitterion to the mica substrate. This issue, of insufficient tension in the sheared PS−X brushes to overcome the zwitterion−mica attachment, is discussed in detail in ref 41.

MA071000N